PCCP

PAPER

View Article Online
View Journal | View Issue

Check for updates

Cite this: *Phys. Chem. Chem. Phys.*, 2018, **20**, 5545

Where's water? The many binding sites of hydantoin†

Sébastien Gruet, *[abc] Cristóbal Pérez, [abc] Amanda L. Steber [abc] and Melanie Schnell *[abc]

Received 22nd September 2017,
Accepted 22nd November 2017

DOI: 10.1039/c7cp06518c

rsc.li/pccp

Prebiotic hydantoin and its complexes with one and two water molecules are investigated using high-resolution broadband rotational spectroscopy in the 2–8 GHz frequency range. The hyperfine structure due to the nuclear quadrupole coupling of the two ^{14}N atoms is analysed for the monomer and the complexes. This characteristic hyperfine structure will support a definitive assignment from low frequency radioastronomy data. Experiments with $H_2{}^{18}O$ provide accurate experimental information on the preferred binding sites of water, which are compared with quantum-chemically calculated coordinates. In the 2-water complexes, the water molecules bind to hydantoin as a dimer instead of individually, indicating the strong water–water interactions. This information provides first insight on how hydantoin interacts with water on the molecular level.

Open Access Article. Published on 28 listopadu 2017. Downloaded on 10.05.2026 21:00:16.
This article is licensed under a Creative Commons Attribution 3.0 Unported Licence.

1 Introduction

The search for prebiotic molecules in the interstellar medium (ISM) has been an ongoing effort of astronomy, astrochemistry, and laboratory spectroscopy for several decades. There is particular interest in simple organic molecules like sugars, amino acids, and their derivates as they will reveal important information about the origin and formation of life. Recently, ground-based observatories have been updated and new ones brought online, such as the Atacama Large Millimeter/submillimeter Array (ALMA), the Robert C. Byrd Greenbank Telescope, and the Institute for Radio Astronomy in the Millimeter Range (IRAM), which provide high-spatial and high-frequency resolution radioastronomic data. This data can be used not only to identify new molecular species in the ISM but also to investigate molecular reaction pathways of previously detected molecules. Once a chemical reaction, by which the discovered molecule can be formed, is proposed, spatial maps of the components of this reaction can be examined in order to judge its likelihood as a contributor to the molecule's occurrence. By systematically checking the feasibility of these reactions through this manner, much insight about the chemistry occurring in interstellar environments can be gleamed.[1,2] In order to identify new molecules and create molecule specific maps, knowledge of the rotational transition frequencies of the molecules of interest is a prerequisite. These can be provided by high-resolution laboratory experiments in the microwave (mw) up to the terahertz regime, using techniques such as THz absorption spectroscopy using solid-state frequency multiplier chains,[3] Fabry–Perot cavity Fourier transform microwave spectroscopy,[4] and chirped pulse Fourier transform microwave (CP-FTMW) spectroscopy.[5]

The cyclic amide hydantoin, or glycolylurea, has many interesting qualities, one of them being its tie to prebiotic chemistry. Hydantoin is a heterocyclic organic compound with the sum formula $C_3H_5N_2O_2$ ($CH_2C(O)NHC(O)NH$) that arises from the reaction of the prebiotic molecules glycolic acid and urea. As urea has already been detected in the interstellar medium (ISM),[6] it is likely that hydantoin could be present, as reactions of urea in the gas phase or on ice grain surfaces with glycolic acid would give rise to the formation of hydantoin. So far, hydantoin has been detected in carbonaceous chondrites together with several amino acids by gas chromatography combined with mass spectrometry.[7] This finding points to reaction pathways connecting hydantoin and amino acids. More recently, laboratory studies on interstellar ice analogues revealed that the hydrolysis of hydantoin, under acidic conditions, can produce small amino acids such as glycine, which is one of the building blocks of life.[8]

Studies providing spectroscopic and structural information on hydantoin are rather limited and mostly dedicated to experiments in the solid phase. These experiments include the previously mentioned studies on ice analogues, a matrix isolation study in which the photochemistry of hydantoin was investigated,[9] and a X-ray crystallography study in which its structure was determined.[10] The vibrational spectra of the

[a] *Deutsches Elektronensychrotron, Notkestrasse 85, D-22607 Hamburg, Germany*
[b] *Institut für Physikalische Chemie, Christian-Albrechts-Universität zu Kiel, Max-Eyth-Strasse 1, D-24118 Kiel, Germany*
[c] *Max-Planck-Institut für Struktur und Dynamic der Materie and The Hamburg Centre for Ultrafast Imaging at the Universität Hamburg, Luruper Chaussee 149, D-22761 Hamburg, Germany. E-mail: melanie.schnell@mpsd.mpg.de*

† Electronic supplementary information (ESI) available. See DOI: 10.1039/c7cp06518c

Open Access Article. Published on 28 listopadu 2017. Downloaded on 10.05.2026 21:00:16.
This article is licensed under a Creative Commons Attribution 3.0 Unported Licence.

normal and enriched isotopologues were also recorded at low resolution in the infrared regime.[11,12] The first high-resolution laboratory spectroscopy study of hydantoin in the gas phase was reported in 2017 using millimeter-wave (mmw) spectroscopy in the frequency range 90 to 370 GHz.[13] Molecular constants for the ground state and two low-lying vibrationally excited states were reported, which can be useful for high frequency radio astronomical observations where molecular vibrationally excited states can be observed. Spectral line catalogues for these states provide useful rest frequencies for searches of hydantoin in interstellar space. Due to rotational transitions corresponding to high J rotational quantum numbers, the unique hyperfine splitting pattern expected for hydantoin, which arises from the nuclear quadrupole coupling of the two nitrogen atoms (^{14}N), was not observed.

In the present work, we investigate hydantoin and its complexes with one and two water molecules using high-resolution broadband rotational spectroscopy. We use the low frequency range (2–8 GHz) of our COMPACT spectrometer to analyse and provide accurate molecular parameters of the nuclear quadrupole coupling hyperfine structure, which can also be useful for the identification of hydantoin in space.[14,15] Every low-J rotational transition will exhibit this uniquely identifying hyperfine splitting. We are also interested in understanding the interactions between hydantoin and water. Indeed, the knowledge of how water binds to such prebiotic precursors is relevant for modeling chemical processes on interstellar ice grains.

2 Experimental and computational details

Rotational spectroscopic measurements were performed with the Hamburg COMPACT spectrometer covering the 2–8 GHz frequency range, which has been described in detail elsewhere.[16] Hydantoin ($C_3N_2O_2H_4$, purchased from Sigma-Aldrich, purity >99%) was placed in a heatable reservoir (a modified Parker General Valve, Series 9) close to the valve orifice and heated to ~180 °C. The resulting vapor pressure was picked up by the backing gas neon and supersonically expanded into the chamber. The jet temperature is estimated to be close to 2 K. For the clusters with water, the neon flowed over an external reservoir containing water, to seed the neon with water. It then passed over the heated hydantoin, before being supersonically expanded into the vacuum chamber. In both cases, the valve operated at a repetition rate of 9 Hz, and 3 bars of neon were used as the backing gas. After the expansion, the molecular jet was polarized with a 4 μs chirp pulse spanning 2–8 GHz. This chirp was generated with an arbitrary waveform generator, amplified with a 300 W traveling wave tube amplifier, and transmitted into the vacuum chamber *via* a horn antenna. Following each excitation pulse, the free induction decay (FID) of the macroscopic ensemble of polarized molecules was recorded for 40 μs. In order to increase the data collection speed and reduce sample consumption, the fast frame capability[17] of the Tektronix digital oscilloscope DPO 71254C was used to collect eight consecutive FIDs in the time domain per gas pulse. This resulted in an effective repetition rate of 72 Hz. For the spectrum of the hydantoin monomer as well as for the hydantoin–$H_2{}^{16}O$ spectrum, 2 million FIDs were coadded. In the hydantoin–$H_2{}^{18}O$ measurements, in which a $H_2{}^{16}O : H_2{}^{18}O$ mixture (2 : 1 ratio) was used, 4 million FIDs were coadded. Fourier transformation of the averaged time domain FID, recorded at point spacings of 10 ps, resulted in the frequency domain rotational spectrum with frequency resolution of 25 kHz.

The transition frequency assignments were carried out using the AABS package,[18] after which the fits were further refined using the SPFIT/SPCAT programs, including parameters to treat the hyperfine structure for the molecule.[19] Comparisons with the quantum-chemical calculations were helpful for predicting the hyperfine splitting due to the two ^{14}N nuclei of hydantoin. A series of programs available on the PROSPE website[20] was used to aid in the assignment of the spectra and determine the experimental structures. The program CORSCL was used to estimate the rotational constants for ^{18}O isotopologues of each complex, while the KRA program was to determine the experimental oxygen-atom positions in the principal axis system (r_s) through the Kraitchman equations, and STRFIT was used to compute the r_0 fits.[21,22] Complementary to the r_s structure, we performed a structural least-squares fit of the experimental moments of inertia of the isotopologues to determine the effective ground state structure (r_0). The initial geometry for the r_0 fits of each complex was taken from *ab initio* calculations.

The experimental results were complemented by and compared with electronic structure calculations. Computations at the B3LYP-D3(BJ)/aug-cc-pVTZ level of theory, which includes dispersion corrections and Becke–Johnson damping,[23] were performed using the Gaussian 09, rev. D.01[24] program suite.

3 Results and discussion

3.1 Rotational spectroscopy of hydantoin

The high-resolution broadband rotational spectrum of the hydantoin monomer is displayed in Fig. 1(a). A limited number of rotational transitions is present in the 2–8 GHz frequency range due to the comparatively large rotational constants of hydantoin. These, among other effects, result in large spacings between the individual groups of transitions. However, hydantoin is an asymmetric-top molecule (near-prolate, with an asymmetry parameter of $\kappa = -0.76$) containing two nitrogen atoms ($I = 1$), which results in rich hyperfine substructure. The bottom panel of Fig. 1(b) shows the hyperfine pattern for the $2_{11} \leftarrow 2_{02}$ b-type rotational transition. The hyperfine structure was modeled with the χ_{ii} (i = a, b, or c) diagonal components of the nuclear quadrupole coupling tensor of each nitrogen atom, taking into account that $\chi_{aa} + \chi_{bb} + \chi_{cc} = 0$.[25] A I_2 coupling scheme was used: the spin I_1 of one nucleus (here the N_1 atom) couples to J to form $F_1 = I_1 + J$, which couples to the vector sum I_2 of the two equivalent spins (N_1 and N_2 atoms) to form $F = F_1 + I_2$.[25]

Open Access Article. Published on 28 listopadu 2017. Downloaded on 10.05.2026 21:00:16.
This article is licensed under a Creative Commons Attribution 3.0 Unported Licence.

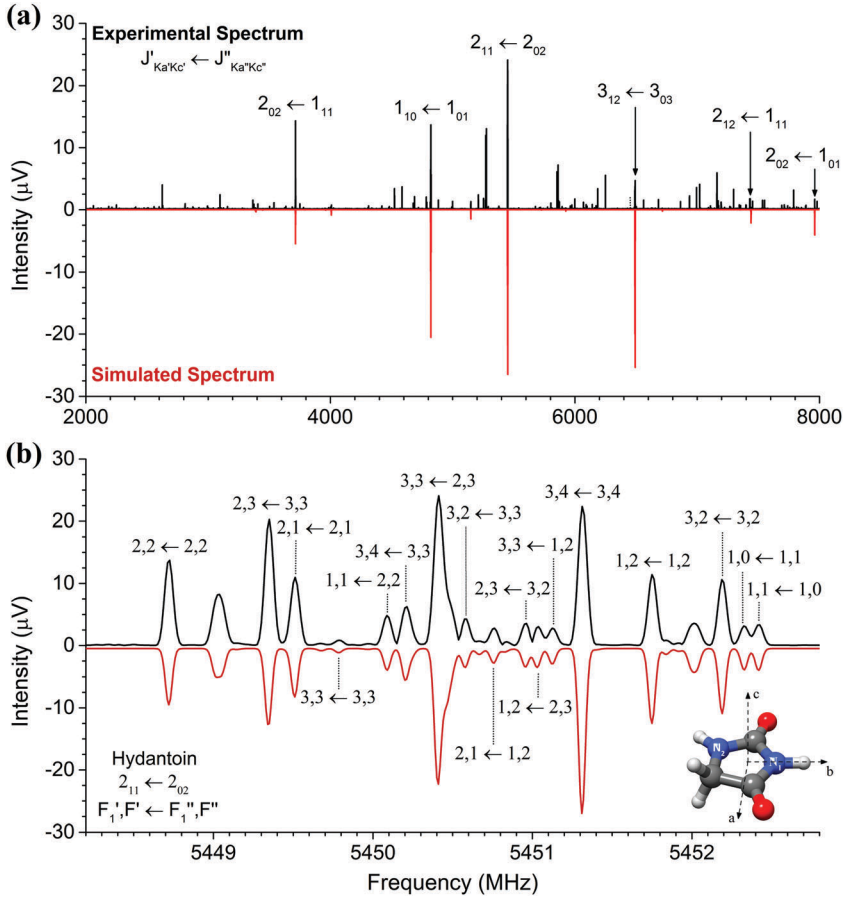

Fig. 1 Panel (a) shows the broadband rotational spectrum of hydantoin (2 million averages), and a zoom of the region of the $2_{11} \leftarrow 2_{02}$ rotational transition is illustrated in panel (b). In both panels, the upper trace (in black) is the experimental spectrum, while the lower trace (in red) corresponds to simulations based on fitted rotational constants of the monomer. Panel (b) illustrates the rich hyperfine structure arising from the nuclear quadrupole coupling of the two ^{14}N nuclei. The hyperfine substructures are labeled with F_1 and F accordingly (see text). The molecular structure including labeling of the two nitrogen atoms is also displayed.

Line splittings due to nuclear quadrupole coupling are inversely proportional to the rotational quantum number J. Because of this, the hyperfine splitting eventually collapses for rotational transitions with increasing J value. In the millimeter-wave study on hydantoin by Ozeki *et al.*,[13] no hyperfine structure was observed because of the high J rotational quantum numbers involved. The low-frequency range of the COMPACT spectrometer probes the lowest rotational transitions, so that, together with the high resolution of the spectrometer, the hyperfine structure is well resolved. We performed a joint fit of the rotational and hyperfine transitions using the SPFIT/SPCAT programs.

The rotational parameters obtained from this fit are summarized in Table 1 and compared with results obtained in the recent mmw spectroscopy study and from quantum-chemical calculations (B3LYP-D3(BJ)/aug-cc-pVTZ). We were unable to perform a global fit of our mw and the previously reported mmw data as only a selected few line frequencies were published in the mmw study. Line lists of the mw rotational transitions including hyperfine structure are given in the ESI.† In our study, inclusion of centrifugal distortion constants into the asymmetric rotor fit were unnecessary. This is different from the mmw study in which high rotational transitions were probed, leading to their use. Even though this is the case, there is very little variation between the two sets of experimental rotational constants. A, B, and C agree to within 10 kHz. The calculated rotational constants agree to within 1% of both experimental methods. This is particularly good considering that the quantum-chemical calculations provide rotational constants for a molecule without considering vibrational zero-point energy corrections. Moreover, good agreement was expected because hydantoin is a decent-size rigid molecule without conformational flexibility.

The nuclear quadrupole coupling constants for the two nitrogen atoms N_1 and N_2 were determined and are shown in Table 1. For a given nucleus, the magnitude of the nuclear quadrupole coupling constants depends on the interaction of the nucleus with the electric field gradient. It thus provides useful information on the character of neighboring chemical bonds. For the two nitrogen atoms N_1 and N_2 (Fig. 1), the nuclear quadrupole coupling constants are different, which points to a difference in their chemical environment. This is indeed the case: N_1 has two adjacent electron withdrawing carbonyl groups, while N_2 has only one neighboring CO group

Open Access Article. Published on 28 listopadu 2017. Downloaded on 10.05.2026 21:00:16.
This article is licensed under a Creative Commons Attribution 3.0 Unported Licence.

Table 1 Experimentally determined spectroscopic constants for the hydantoin monomer (this work) in comparison with the millimeter-wave spectroscopy study[13] and the results from quantum-chemical calculations (B3LYP-D3(BJ)/aug-cc-pVTZ). For the nuclear quadrupole coupling constants, the numbers in parentheses refer to the two nitrogen nuclei

Parameters	Parent fit (this work)	Parent fit (mmw)[13]	Calc.
A (MHz)	6537.73154(80)	6537.73998(70)	6570.35
B (MHz)	2291.37309(21)	2291.37582(57)	2289.88
C (MHz)	1716.47119(31)	1716.471265(67)	1716.35
Δ_J (kHz)		0.095338(167)	
Δ_{JK} (kHz)		0.15923(69)	
Δ_K (kHz)		2.25266(83)	
δ_J (kHz)		0.025701(83)	
δ_K (kHz)		0.28008(144)	
$\chi_{aa}(1)$ (MHz)	1.6316(57)		1.671
$\chi_{bb-cc}(1)$ (MHz)	5.227(20)		5.370
$\chi_{ab}(1)$ (MHz)	[0.092]		0.092
$\chi_{aa}(2)$ (MHz)	2.5927(43)		2.753
$\chi_{bb-cc}(2)$ (MHz)	6.935(16)		7.439
$\chi_{ab}(2)$ (MHz)	[−0.223]		−0.223
N_{lines}	114	161	
RMS (kHz)	5.3	39	
$\mu_a/\mu_b/\mu_c$ (D)			0.2/2.7/0
No. of lines ($a/b/c$)	27/87/0		

and a CH_2 group. This results in N_2 having a higher electron density than N_1 and thus larger χ_{ii} values.

3.2 Hydantoin–water complexes

3.2.1 Hydantoin–H_2O complexes. In order to elucidate the preferred binding positions of water to hydantoin, we recorded the rotational spectrum of hydantoin with water (see Experimental section). As can be seen from the top panel of Fig. 2, the experimental spectrum is much richer than for the hydantoin monomer. This allowed for five hydantoin–water complexes to be assigned: three 1-water complexes and two 2-water complexes. Hydantoin offers several qualitatively different binding positions for water molecules. The multiple carbonyl-oxygen atoms are good hydrogen-bond acceptors, while the amino (NH) groups are good hydrogen-bond donors. The heterocyclic geometry results in five binding positions for water. The three lowest energy structures for the 1-water complexes are shown in Fig. 3 (top row), and they are labeled 1w-I, 1w-II, and 1w-III. They each allow for networks involving hydrogen bonds with both a CO and an NH group. This results in a hydrogen bonded six-membered ring. As the three complexes are close in energy, all three were experimentally observed (see Fig. 3). Our quantum-chemical calculations also revealed two other hydantoin–water complexes. The first consisted of only one hydrogen bond to a carbonyl oxygen atom. This one is significantly higher in energy ($\approx$9.8 kJ mol^{-1}) and was not observed in the rotational

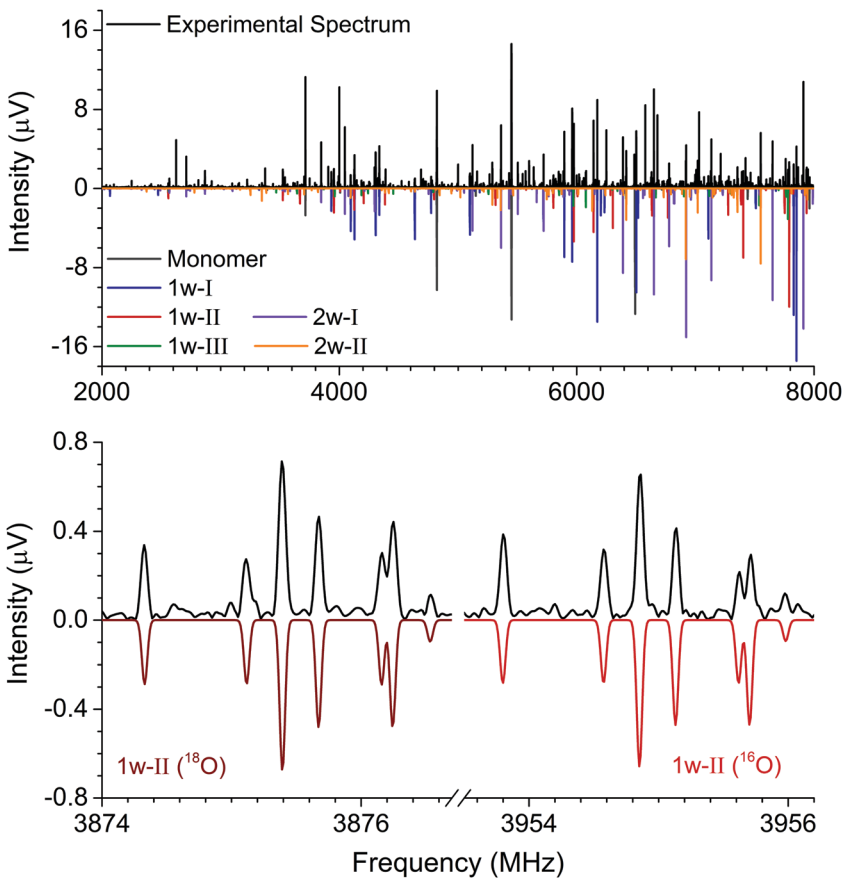

Fig. 2 The top panel shows the broadband rotational spectrum of hydantoin–water (4 million averages). Five complexes were identified, as illustrated by the color code for the fitted spectra given in the lower trace. The bottom panel shows an inset of the $1_{11} \leftarrow 0_{00}$ transition of the 1w-II complex. The left side of the spectrum displays the transition for the $H_2{}^{18}O$ spectrum, while the right side shows the same transition for the $H_2{}^{16}O$ spectrum.

 This journal is © the Owner Societies 2018

Open Access Article. Published on 28 listopadu 2017. Downloaded on 10.05.2026 21:00:16.
This article is licensed under a Creative Commons Attribution 3.0 Unported Licence.

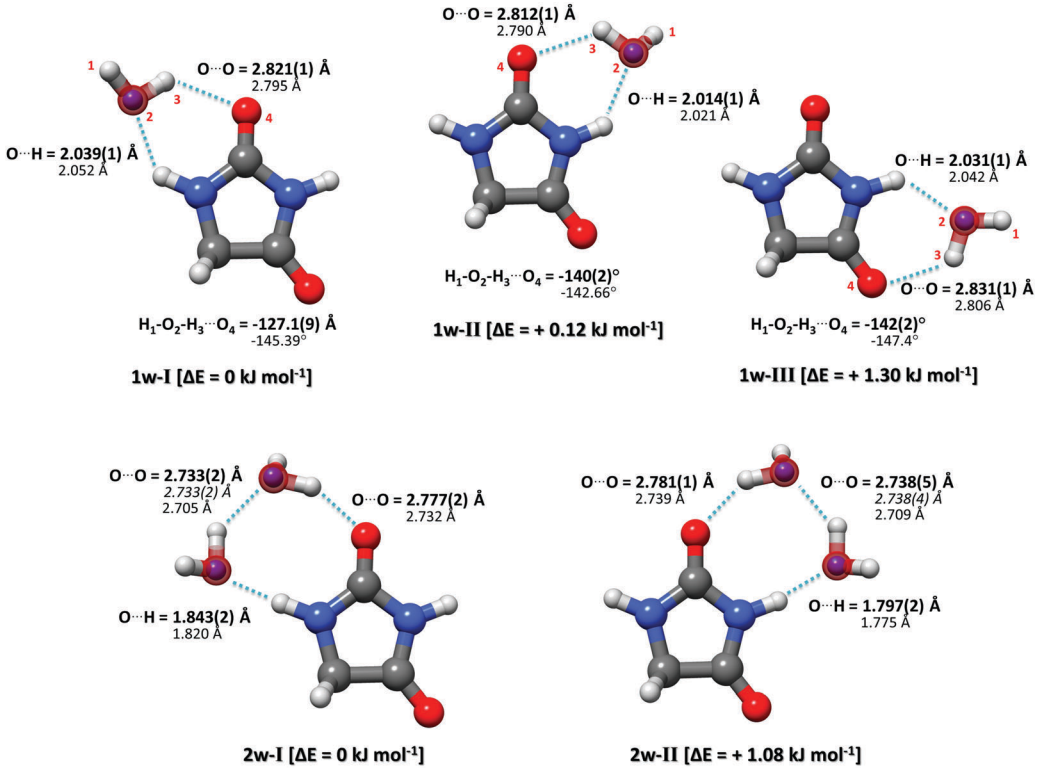

Fig. 3 Complexes of hydantoin with one (upper row) and two water molecules (lower row). The experimentally determined r_s oxygen positions of the water molecules are displayed as purple spheres. The underlying structures are experimentally determined r_0 structures. The bold parameters are from the r_0 experimental structure, the italicized values are the O–O distances determined from the r_s experimental structures, and the non-bold values are from the calculated structures (B3LYP-D3(BJ)/aug-cc-pVTZ level of theory). The relative calculated energies were obtained from the quantum chemical calculations and are zero-point vibrational energy corrected.

spectrum. A potential fifth structure, where water only binds to the NH group containing N_2, was considered to be too high in energy to be relevant for this study.

The rotational constants of the experimentally observed complexes 1w-I, 1w-II, and 1w-III are summarized in Table 2. Their values are sufficiently different to unambiguously differentiate and assign the individual complexes based solely on a comparison between the experimental and *ab initio* rotational constants. For further elucidation of the assignments, the types of rotational transitions assigned (*a*-, *b*-, or *c*-type) were compared with the calculated dipole moment components. Complexes 1w-I and 1w-II are predicted to have a strong μ_b value as well as a μ_a component, and both types of transitions were assigned for the two complexes. Complex 1w-III, however, is predicted to only have a μ_b component, which agrees with our experimental observations. Note that for all three complexes,

Table 2 Experimentally determined spectroscopic constants for hydantoin–H_2O complexes in comparison with results of quantum-chemical calculations (B3LYP-D3(BJ)/aug-cc-pVTZ). For the nuclear quadrupole coupling constants, the numbers in parentheses refer to the two nitrogen nuclei

Parameters	1w-I	Calc.	1w-II	Calc.	1w-III	Calc.
A (MHz)	5029.76179(63)	5077.85	2944.64549(47)	2969.01	2956.01125(78)	2987.27
B (MHz)	1135.03113(20)	1140.42	1520.96485(56)	1527.09	1507.54475(93)	1510.23
C (MHz)	932.88647(16)	938.13	1010.39251(44)	1016.37	1005.70153(76)	1010.68
Δ_J (kHz)	0.1305(62)		0.300(23)		0.305(42)	
δ_J (kHz)	—		0.1039(54)		—	
$\chi_{aa}(1)$ (MHz)	1.7100(73)	1.763	1.4634(59)	1.457	1.541(23)	1.641
$\chi_{bb-cc}(1)$ (MHz)	5.185(10)	5.309	4.873(11)	4.892	4.488(27)	4.462
$\chi_{ab}(1)$ (MHz)	[0.136]	0.136	[0.327]	0.327	[−0.251]	−0.251
$\chi_{aa}(2)$ (MHz)	2.0814(62)	2.177	2.5916(44)	2.715	2.137(10)	2.365
$\chi_{bb-cc}(2)$ (MHz)	6.7832(76)	7.070	6.7080(92)	7.247	7.346(14)	7.870
$\chi_{ab}(2)$ (MHz)	[−0.595]	−0.595	[0.161]	0.161	[−0.249]	−0.249
N_{lines}	179		181		86	
RMS (kHz)	5.0		7.5		9.2	
$\lvert\mu_a\rvert/\lvert\mu_b\rvert/\lvert\mu_c\rvert$ (D)		1.1/1.2/0.9		1.0/3.0/0.8		0.7/3.1/0.8
No. of lines (a/b/c)	89/90/0		32/149/0		0/87/0	

Open Access Article. Published on 28 listopadu 2017. Downloaded on 10.05.2026 21:00:16.
This article is licensed under a Creative Commons Attribution 3.0 Unported Licence.

we do not observe an indication of *c*-type transitions or internal motion of the water molecule. The formation of two relatively strong hydrogen bonds prevents the water monomer from exhibiting internal dynamics.

To obtain experimental structure information and to further support the assignment, we performed a series of experiments in which the water sample was comprised of a 2 : 1 ratio of $H_2{}^{16}O : H_2{}^{18}O$. The analysis of this new dataset yielded three additional rotational assignments (one per cluster). The tables reporting rotational parameters for these three new complexes are provided in the ESI.† By isotopically substituting the $H_2{}^{16}O$ with an $H_2{}^{18}O$, induced changes in the moments of inertia of the cluster can be used for determining the oxygen-atom positions in the principal axis system through the Kraitchman equations.[21] This renders the so-called substitution structure (r_s). Although the r_s structure is of common application in rotational spectroscopy, it presents limitations when determining structural parameters. This is particularly limiting when the isotopic information is sparse and the substituted atom lies near an inertial axis where vibrational contributions can play an important role. Theoretical calculations for the three observed complexes show that the water monomer is located near or in the hydantoin *ab* inertial plane. This was corroborated through the imaginary values of the *c* coordinate for the oxygen atom upon isotopic substitution, which were set to zero for structural comparisons.

Complementary to the r_s structure, we performed a structural least-squares fit of the experimental moments of inertia of the isotopologues to determine the effective ground state structure (r_0). The initial geometry for the r_0 fits of each complex was taken from *ab initio* calculations. The relevant structural parameters are shown in Fig. 3 for all three clusters. An important feature to consider is the degree of planarity the structures exhibit upon water complexation. A first indication of the non-planarity of the clusters comes from the inertial defect, defined as $\Delta_c = I_c - I_a - I_b$. This parameter quantifies the mass distribution out of the *ab* inertial plane. For the hydantoin monomer this value is −3.430102(58) uÅ^2. This indicates that even in the monomer, there are small contributions from the out-of-plane atoms: the hydrogen atoms in the CH_2 group. The inertial defect for the water complexes are −3.99647(12) uÅ^2, −3.72083(25) uÅ^2 and −3.68579(43) uÅ^2 for 1w-I, 1w-II and 1w-III respectively. These values are slightly larger than those for the monomer indicating more non-planarity in the structure. These values essentially remain unchanged upon $H_2{}^{18}O$ substitution showing that the oxygen atoms lie in the *ab* inertial plane, thus indicating that the increased non-planarity must be due to at least one proton of the water. This is indeed the case, and the r_0 structural fit allowed us to determine that the dangling hydrogen orientation is out of the plane. By fitting the dihedral angle corresponding to this non-planarity (H_1–O_2–H_3–O_4), our results show that the structure for complex 1w-I has the smallest dihedral angle at −127.1(9)°, while complex 1w-III has the largest angle at −142.2(2)°. This agrees with the changes in the inertial defects for each of these structures. This is also in good agreement with the calculated structures. For a set of similar systems (*i.e.* uracil–water and thymine–water complexes), the authors were forced to fix this dihedral to 140° in order to obtain a r_0 fit.[26]

3.2.2 Hydantoin–$(H_2O)_2$ complexes. Knowing where the water molecule preferred to bind for the 1-water complexes, an intriguing question as to where a second water molecule would preferentially bind was raised. It has been shown in a number of investigations that in microsolvated systems water–water interactions typically dominate in complex formation. This phenomenon results in complex structures that can be understood to be comprised of a water cluster and the solvate. It is observed that both the solvate and the water clusters adjust their structures to achieve optimum binding, such as the complexes involving camphor,[27] β-propiolactone,[28] and the 12-crown-4 ether.[29] If the solvate molecule offers a number of strong binding positions for water, like in the case of hydantoin, it can be envisioned that the situation can be different and that the water molecules bind separately to the solvate. In addition, cooperativity effects might play a role.

In our broadband spectra, we observed rotational signatures of two species with rotational constants that fit to what we would expect for the size of hydantoin–$(H_2O)_2$ complexes. One spectrum is dominated by a-type transitions, while the second mainly consists of b-type transitions. Both spectra could be fit individually to asymmetric rotor Hamiltonians including the nuclear quadrupole coupling of two nitrogen nuclei. Again, no indication of water tunneling in the complexes was observed. The resulting rotational and nuclear quadrupole coupling constants are summarized in Table 3. The energy difference between the two structures amounts to ∼1 kJ mol^{-1}. Our calculations predicted an additional 2-water complex involving the ''water–dimer'' unit, which binds to the NH group containing N_1 and the CO group neighboring the CH_2 group, similar to the 1w-III complex. This is predicted to be about 4.6 kJ mol^{-1} higher in energy than complex I, and it was not observed in our spectrum. A fourth complex, where the two water molecules

Table 3 Experimentally determined spectroscopic constants for hydantoin–$(H_2O)_2$ complexes in comparison with results of quantum-chemical calculations (B3LYP-D3(BJ)/aug-cc-pVTZ). For the nuclear quadrupole coupling constants, the numbers in parentheses refer to the two nitrogen nuclei

Parameters	2w-I	Calc.	2w-II	Calc.
A (MHz)	2938.0518(12)	2977.06	2120.22255(63)	2125.42
B (MHz)	754.55686(17)	765.55	946.67424(56)	969.57
C (MHz)	604.47571(17)	613.12	658.71724(43)	670.81
Δ_J (kHz)	0.0621(31)		0.1959(77)	
Δ_{JK} (kHz)	—		−0.689(37)	
Δ_K (kHz)	4.05(28)		2.408(87)	
δ_J (kHz)	—		0.0529(66)	
$\chi_{aa}(1)$ (MHz)	1.7000(73)	1.771	1.2380(73)	1.167
$\chi_{bb-cc}(1)$ (MHz)	5.181(13)	5.287	4.625(14)	4.620
$\chi_{ab}(1)$ (MHz)	[0.154]	0.154	[0.565]	0.565
$\chi_{aa}(2)$ (MHz)	1.5713(66)	1.828	2.5276(57)	2.638
$\chi_{bb-cc}(2)$ (MHz)	6.500(10)	6.730	6.750(11)	7.272
$\chi_{ab}(2)$ (MHz)	[−0.792]	−0.792	[0.188]	0.188
N_{lines}	218		135	
RMS (kHz)	5.9		7.5	
$\lvert\mu_a\rvert/\lvert\mu_b\rvert/\lvert\mu_c\rvert$ (D)		1.4/0.8/0		1.0/2.9/0.1
No. of lines (a/b/c)	131/87/0		22/115/0	

Open Access Article. Published on 28 listopadu 2017. Downloaded on 10.05.2026 21:00:16.
This article is licensed under a Creative Commons Attribution 3.0 Unported Licence.

bind separately to the NH and CO groups of hydantoin, is more than 11 kJ mol^{-1} higher in energy.

Like in the case of the hydantoin–H_2O complexes, we also investigated the 2-water complexes with $H_2{}^{18}O$. Unlike the 1-water complexes where there is only one position for the insertion of $H_2{}^{18}O$, here we have two possibilities, $H_2{}^{16}O$–$H_2{}^{18}O$ and $H_2{}^{18}O$–$H_2{}^{16}O$. Due to their different location with respect to the cluster's center of mass, their single substitution gives rise to two new, separated rotational spectra. The rotational parameters for these four new spectra, two per cluster, are shown in the ESI.† The r_0 experimental parameters were also obtained in both cases from a fit to nine moments of inertia from three different isotopologues. The relevant experimental structural parameters are compared with results from B3LYP-D3(BJ)/aug-cc-pVTZ calculations (lower values) in Fig. 3. The structural analysis for both complexes revealed that the two water molecules form a unit (similar to the water dimer) in which one water moiety forms a hydrogen bond with a CO group and the second water monomer forms a hydrogen bond with the neighboring NH group. This results in hydrogen bonded eight-membered rings that further stabilize the cluster and involve the formation of three hydrogen bonds.

Interesting structural differences are observed when comparing the bonding distances of our clusters to those of the bare water dimer and/or other molecular clusters that include two water molecules. These are dictated by cooperative effects. The presence of one hydrogen bond increases the unequal charge distribution in water and leads to further polarisation. This can make the remaining part of water more susceptible to additional hydrogen bonds, especially when polar groups are present and substantially modify the strength of a given hydrogen bond. In the case of hydantoin, a clear indication of cooperativity can be observed when looking at the $C{=}O\cdots O_{water}$ distances. While for the 1-water clusters the distances are all above 2.8 Å, a clear shortening to 2.777(2) Å and 2.781(1) Å for 2w-I and 2w-II respectively is seen. Furthermore, it is interesting to compare the O_{water}–O_{water} distance of the two water molecules of complexes I and II with the O_{water}–O_{water} distances observed for the free water dimer and other 2-water molecule complexes. At 2.733(2) Å (complex I) and 2.738(4) Å (complex II), the O–O distances are significantly shorter than in the isolated $(H_2O)_2$ (2.98(4) Å).[30] They are also about 0.1 Å shorter than the O–O distances for a number of other molecular complexes with two water molecules: biphenyl 2-carboxaldehyde–$(H_2O)_2$ (2.852(2) Å),[31] camphor–$(H_2O)_2$ (2.821(2) Å for complex 2w(I) and 2.837(1) Å for complex 2w(II)),[27] β-propiolactone–$(H_2O)_2$ (2.85(1) Å),[28] or the 12-crown-4 ether with 2.779(3) Å.[29] The observed shortening can be attributed to a larger donor character of the –NH group of hydantoin with respect to aliphatic hydrogens as those in the systems mention above. This marked acidity contributes to the strengthening of the stability of the overall hydrogen network, which manifests itself as shorter interaction distances.

4 Summary and conclusions

In summary, we used broadband rotational spectroscopy to study the prebiotic molecule hydantoin and its complexes with up to two water molecules. Hydantoin is a cyclic molecules, offering two amide groups and thus a number of possibilities for the formation of hydrogen bonds with water molecules. We observed three qualitatively different complexes of hydantoin with one water molecule, all within relative energies less than 1.5 kJ mol^{-1} of each other. Each water molecule forms two hydrogen bonds, one with the CO and one with the NH group, resulting in a hydrogen-bonded six-membered ring. For the complexes with two water molecules, there is evidence to suggest that water forms a dimer which then binds to one of the amide groups, forming an hydrogen-bonded eight-membered ring. This illustrates the dominance of water–water interactions. The structural assignment of the water complexes was supported by using $H_2{}^{18}O$-enriched samples to determine both the substitution (r_s) and the effective ground state (r_0) structures as well as by analysis of the hyperfine structure arising from the two amide nitrogen atoms in hydantoin. This structural analysis allowed an accurate characterization of the structure of the clusters that were compared to other water aggregates where structural information was available. Cooperativity effects explain the significantly shorter O–O distances observed for the 2-water complexes compared to those observed in the free water dimer or in other complexes of polar molecules with two water molecules. This showcases the hydrogen bond donor character of the –NH in amides.

Due to its unique hyperfine patterns, hydantoin offers itself as a likely candidate to be identified in the ISM, as no other molecule would exhibit the same hyperfine splitting pattern. As a consequence, a small number of rotational transitions would be sufficient for its unambiguous assignment. The identification of this molecule in the ISM has larger implications than just the discovery of another molecule. Its formation is dependent upon urea, which has already been identified in the ISM, and it can go on to form the amino acid glycine which is an important step to the evolution of life. Interactions of hydantoin with water have been shown. These are an important first step to understanding how water would impact the chemistry that hydantoin would be involved in, if it were created through chemical reactions on ice grains.

Conflicts of interest

There are no conflicts to declare.

Acknowledgements

This work was performed as part of our activities within the framework of the ERC Starting grant 'Astrorot', grant agreement number 638027. It has also been supported by the Deutsche Forschungsgemeinschaft within the priority program SPP1807 (SCHN1280/4-1) and by the excellence cluster 'The Hamburg Centre for Ultrafast Imaging – Structure, Dynamics and Control of Matter at the Atomic Scale' of the Deutsche Forschungsgemeinschaft *via* a Louise Johnson Fellowship for A. L. S. Open Access funding provided by the Max Planck Society.

Open Access Article. Published on 28 listopadu 2017. Downloaded on 10.05.2026 21:00:16.
This article is licensed under a Creative Commons Attribution 3.0 Unported Licence.

References

1 E. Herbst and E. F. van Dishoeck, *Annu. Rev. Astron. Astrophys.*, 2009, **47**, 427–480.
2 M. Bonfand, A. Belloche, K. M. Menten, R. T. Garrod and H. S. P. Müller, *Astron. Astrophys.*, 2017, **604**, A60.
3 G. Chattopadhyay, E. Schlecht, J. S. Ward, J. J. Gill, H. H. S. Javadi, F. Maiwald and I. Mehdi, *IEEE Trans. Microwave Theory Tech.*, 2004, **52**, 1538–1547.
4 T. J. Balle and W. H. Flygare, *Rev. Sci. Instrum.*, 1981, **52**, 33–45.
5 G. G. Brown, B. C. Dian, K. O. Douglass, S. M. Geyer, S. T. Shipman and B. H. Pate, *Rev. Sci. Instrum.*, 2008, **79**, 053103.
6 A. J. Remijan, L. E. Snyder, B. A. McGuire, H.-L. Kuo, L. W. Looney, D. N. Friedel, G. Y. Golubiatnikov, F. J. Lovas, V. V. Ilyushin, E. A. Alekseev, S. F. Dyubko, B. J. McCall and J. M. Hollis, *Astrophys. J.*, 2014, **783**, 77.
7 A. Shimoyama and R. Ogasawara, *Origins Life Evol. Biospheres*, 2002, **32**, 165–179.
8 P. de Marcellus, M. Bertrand, M. Nuevo, F. Westall and L. Le Sergeant d'Hendecourt, *Astrobiology*, 2011, **11**, 847–854.
9 G. O. Ildiz, C. M. Nunes and R. Fausto, *J. Phys. Chem. A*, 2013, **117**, 726–734.
10 F.-L. Yu, C. H. Schwalbe and D. J. Watkin, *Acta Crystallogr., Sect. C: Cryst. Struct. Commun.*, 2004, **60**, o714–o717.
11 Y. Saito and K. Machida, *Bull. Chem. Soc. Jpn.*, 1978, **51**, 108–112.
12 G. O. Ildiz, I. Boz and O. Unsalan, *Opt. Spectrosc.*, 2012, **112**, 665–670.
13 H. Ozeki, R. Miyahara, H. Ihara, S. Todaka, K. Kobayashi and M. Ohishi, *Astron. Astrophys.*, 2017, **600**, A44.
14 D. P. Zaleski, N. A. Seifert, A. L. Steber, M. T. Muckle, R. A. Loomis, J. F. Corby, J. Oscar Martinez, K. N. Crabtree, P. R. Jewell, J. M. Hollis, F. J. Lovas, D. Vasquez, J. Nyiramahirwe, N. Sciortino, K. Johnson, M. C. McCarthy, A. J. Remijan and B. H. Pate, *Astrophys. J., Lett.*, 2013, **765**, L10.
15 B. A. McGuire, A. M. Burkhardt, C. N. Shingledecker, S. V. Kalenskii, E. Herbst, A. J. Remijan and M. C. McCarthy, *Astrophys. J., Lett.*, 2017, **843**, L28.
16 D. Schmitz, V. A. Shubert, T. Betz and M. Schnell, *J. Mol. Spectrosc.*, 2012, **280**, 77–84.
17 C. Perez, S. Lobsiger, N. A. Seifert, D. P. Zaleski, B. Temelso, G. C. Shields, Z. Kisiel and B. H. Pate, *Chem. Phys. Lett.*, 2013, **571**, 1–15.
18 Z. Kisiel, L. Pszczółkowski, I. R. Medvedev, M. Winnewisser, F. C. De Lucia and E. Herbst, *J. Mol. Spectrosc.*, 2005, **233**, 231–243.
19 H. M. Pickett, *J. Mol. Spectrosc.*, 1991, **148**, 371–377.
20 Z. Kisiel, in *Spectroscopy from Space*, ed. J. Demaison, K. Sarka and E. A. Cohen, Springer, Dordrecht, 2001, pp. 91–106.
21 J. Kraitchman, *Am. J. Phys.*, 1953, **21**, 17–24.
22 Z. Kisiel, *J. Mol. Spectrosc.*, 2003, **218**, 58–67.
23 S. Grimme, S. Ehrlich and L. Goerigk, *J. Comput. Chem.*, 2011, **32**, 1456–1465.
24 M. J. Frisch, G. W. Trucks, H. B. Schlegel, G. E. Scuseria, M. A. Robb, J. R. Cheeseman, G. Scalmani, V. Barone, B. Mennucci, G. A. Petersson, H. Nakatsuji, M. Caricato, X. Li, H. P. Hratchian, A. F. Izmaylov, J. Bloino, G. Zheng, J. L. Sonnenberg, M. Hada, M. Ehara, K. Toyota, R. Fukuda, J. Hasegawa, M. Ishida, T. Nakajima, Y. Honda, O. Kitao, H. Nakai, T. Vreven, J. A. Montgomery, Jr., J. E. Peralta, F. Ogliaro, M. Bearpark, J. J. Heyd, E. Brothers, K. N. Kudin, V. N. Staroverov, R. Kobayashi, J. Normand, K. Raghavachari, A. Rendell, J. C. Burant, S. S. Iyengar, J. Tomasi, M. Cossi, N. Rega, J. M. Millam, M. Klene, J. E. Knox, J. B. Cross, V. Bakken, C. Adamo, J. Jaramillo, R. Gomperts, R. E. Stratmann, O. Yazyev, A. J. Austin, R. Cammi, C. Pomelli, J. W. Ochterski, R. L. Martin, K. Morokuma, V. G. Zakrzewski, G. A. Voth, P. Salvador, J. J. Dannenberg, S. Dapprich, A. D. Daniels, O. Farkas, J. B. Foresman, J. V. Ortiz, J. Cioslowski and D. J. Fox, *Gaussian 09 Revision D.01*, Gaussian Inc., Wallingford CT, 2009.
25 W. Gordy and R. L. Cook, *Microwave Molecular Spectra*, Wiley, 1984.
26 J. C. López, J. L. Alonso, I. Peña and V. Vaquero, *Phys. Chem. Chem. Phys.*, 2010, **12**, 14128–14134.
27 C. Pérez, A. Krin, A. L. Steber, J. C. López, Z. Kisiel and M. Schnell, *J. Phys. Chem. Lett.*, 2016, **7**, 154–160.
28 C. Pérez, J. L. Neill, M. T. Muckle, D. P. Zaleski, I. Peña, J. C. Lopez, J. L. Alonso and B. H. Pate, *Angew. Chem., Int. Ed.*, 2015, **54**, 979–982.
29 C. Pérez, J. C. López, S. Blanco and M. Schnell, *J. Phys. Chem. Lett.*, 2016, **7**, 4053–4058.
30 T. R. Dyke, K. M. Mack and J. S. Muenter, *J. Chem. Phys.*, 1977, **66**, 498–510.
31 S. R. Domingos, C. Pérez and M. Schnell, *J. Chem. Phys.*, 2016, **145**, 161103.